Colloid Polym Sci (2009) 287:961–967
DOI 10.1007/s00396-009-2052-x

ORIGINAL CONTRIBUTION

A molecular dynamics approach to examine the kinetics of the capillary imbibition of a polymer at nanoscale

S. Ahadian · Y. Kawazoe

Received: 2 February 2009 / Revised: 30 April 2009 / Accepted: 6 May 2009 / Published online: 15 May 2009

Abstract A molecular dynamics (MD) approach was employed to simulate the imbibition of a designed nanopore by a polymer. The length of imbibition as a function of time for various interactions between the polymer and the pore wall was recorded for this system (i.e., polymer and nanopore). By and large, the kinetics of imbibition was successfully described by the Lucas–Washburn (LW) equation, although deviation from it was observed in some cases. This nonuniformity contributes to the neglect of the dynamic contact angle (DCA) in the LW equation. Two commonly used models (i.e., hydrodynamic and molecular–kinetic models) were thus employed to calculate the DCA. It is demonstrated that none of the evaluated models is able to justify the simulation results in which are not in good agreement with the simple LW equation. Further investigation of the MD simulation data revealed an interesting fact that there is a direct relationship between the wall–polymer interaction and the speed of the capillary imbibition. More evidence to support this claim will be presented.

Keywords Nanopore imbibition of polymers · Molecular dynamics simulation · Lucas–Washburn equation · Dynamic contact angle · Hydrodynamic model · Molecular–kinetic model

Introduction

Confinement of matter that imposes spatial constraints on molecules does open avenues to novel applications [1]. In the case of polymers, with development of nanofabrication processes, the dynamics of confined polymers has significant technological implications [2–4]. To characterize this phenomenon, one approach is to measure the rate of penetration of the liquid into the medium, which is then modeled as a bundle of uniform capillaries. A schematic diagram of this process is shown in Fig. 1. On a macroscopic scale, a commonly used equation, i.e., the Lucas–Washburn (LW) equation, of such flow processes was proposed almost a century ago [5, 6]. The LW equation relates the length of liquid penetration in a straight-line capillary H to the permeation time t, the capillary radius R, the viscosity and surface tension of the liquid, η and γ_{lv}, respectively, and the contact angle θ between the liquid and the capillary wall as follows:

$$H^2 = \left(\frac{R\gamma_{lv}\cos\theta}{2\eta}\right)t \tag{1}$$

The applicability of the LW equation has been tested for modeling liquid flow in nanopores [7, 8]. To derive this equation, it is assumed that the contact angle does not change during the imbibition process. However, this assumption is not correct in general since the contact angle corresponds to the moving wetting line, and its value therefore depends on the wetting-line velocity [9]. Hence, modification of the LW equation is essential to take the velocity-dependent dynamic contact angle (DCA) into account. To estimate the DCA, various models of wetting-line movement can be used, such as those based on hydrodynamics [10, 11], molecular kinetics [12, 13], or phenomenology [14], in which DCA is a function of wetting-line velocity (i.e., dH/dt). In this study, we focus on the hydrodynamic and molecular–kinetic (MK) models since they are among the top-cited models in the literature.

S. Ahadian (✉) · Y. Kawazoe
Institute for Materials Research (IMR), Tohoku University,
Tohoku, Sendai,
980-8577, Japan
e-mail: ahadian@imr.edu
e-mail: samad_ahadian@yahoo.com

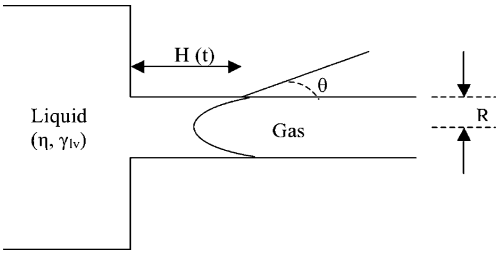

Fig. 1 A schematic representation of flow of a liquid through a nanochannel having the radius R. (Note that the time-dependent height of imbibition is showed by $H(t)$ for the liquid, which has the viscosity and the surface tension η and γ_{lv}, respectively. In addition, ideally, the meniscus of the liquid has a parabolic velocity profile and makes a contact angle (θ) with the tube wall.)

In the context of the hydrodynamic model, the first analysis was proposed by Voinov [15]. Later treatments differ in some detail. However, they recovered an equation of essentially the same form. To our knowledge, the most complete analysis is the Cox equation [10] as follows:

$$\theta_d = \left(\theta_e^3 + 9A\frac{\eta}{\gamma_{lv}}\frac{dH}{dt}\right)^{1/3} \tag{2}$$

and $A=\ln(R/s)$, where R is the characteristic length of the system, s is the slip length, and θ_d and θ_e denote the dynamic and equilibrium contact angles, respectively. In the case of the capillary penetration phenomenon, the characteristic length R is the capillary radius, and the slip length s is the distance from the capillary wall that defines a region where the continuum description of fluid motion tends to break down [16]. The value of slip length should be in the order of molecular dimensions [17]. However, in practice, the quantity s is usually treated as an adjustable parameter. The modified version of the LW equation, including the effect of the DCA on the penetration kinetics, is as follows:

$$\frac{dH}{dt} = \left(\frac{R\gamma_{lv}\cos\theta_d}{4\eta H}\right) \tag{3}$$

The hydrodynamic model considers the dynamic wetting process to be dominated by the viscous dissipation of the liquid, assuming that the bulk viscous friction is the main resistance force for the three-phase wetting-line motion. It is worthwhile to note that the hydrodynamic model does not take the characteristics of the solid surface into account, which is the main limitation of the model. Additionally, the physical meaning of the parameters in this model is not unambiguous [18].

In contrast to the hydrodynamic model, the MK model, which was first suggested by Cherry et al. [19] and Blake et al. [12], excludes the viscous dissipation and takes the solid surface characteristics into account [20] such that the energy dissipation occurs only at the moving contact line. According to this model, the macroscopic behavior of the wetting line depends on the overall statistics of the individual molecular displacements that occur within the three-phase zone, i.e., the microscopic region where the fluid/fluid interface meets the solid surface. The velocity of the wetting line is characterized by K^0, the natural frequency of the molecular displacements, and λ, their average length. In simple cases, λ stands for the distance between two neighboring adsorption sites on the solid surface. Assuming the driving force for the wetting line to be the out-of-balance surface tension force $\gamma_{lv}(\cos\theta_e - \cos\theta_d)$ and using the Eyring activated-rate theory for transport in liquids gives a relationship between θ_d and the velocity of the wetting line dH/dt:

$$\frac{dH}{dt} = 2K^0\lambda\sinh\left[\frac{\gamma_{lv}(\cos\theta_e - \cos\theta_d)}{2nk_BT}\right] \tag{4}$$

where n is the number of adsorption sites per unit area, k_B is the Boltzmann constant, and T is the temperature. For small arguments of the sinh function, which occur when the driving force is small (e.g., near equilibrium, close to the critical temperature, or at high temperatures), the above equation simplifies to:

$$\frac{dH}{dt} = \frac{K^0\lambda}{nk_BT}[\gamma_{lv}(\cos\theta_e - \cos\theta_d)] \tag{5}$$

or

$$\frac{dH}{dt} = \frac{1}{\zeta}[\gamma_{lv}(\cos\theta_e - \cos\theta_d)] \tag{6}$$

where $\zeta = nk_BT/K^0\lambda$ is effectively the coefficient of the wetting-line friction and is a function of the liquid viscosity and the interaction between the liquid and the solid surface [21]. By combining Eqs. 6 and 3, we obtain the desired equation for the capillary imbibition as follows:

$$\gamma_{lv}\left[\cos\theta_e - \frac{\zeta}{\gamma_{lv}}\left(\frac{dH}{dt}\right)\right] = \frac{4}{R}\eta H\frac{dH}{dt} \tag{7}$$

While the experimentally determined values of λ are usually in the order of molecular dimensions, those for K^0 can vary widely and generally decrease with increasing the viscosity of liquid. Moreover, there is no definitive way of predicting the values of λ, K^0, and ζ for a given solid–liquid system and therefore predicting the dynamic wetting behavior from independently measured quantities. As a consequence, λ and K^0 (or ζ) are usually treated as adjustable parameters and should be obtained from experimental results by the curve-fitting procedure. Another problem intrinsic to the MK model is that there is no link to the wider hydrodynamics of the system [22].

In order to study the flow behavior of fluids inside nanochannels, one can exploit the benefits of the molecular dynamics (MD) simulation approach, which serves as a powerful tool to explore the molecular details of phenomena. To our knowledge, the first analysis of the capillary imbibition at nanoscale using MD simulation was reported by Martic et al. [13, 23, 24]. They verified the validity of the MK model along with the LW equation to explain the dynamics of the capillary imbibition at nanoscale. Recently, a general model to demonstrate the fluid flow in nanopores has been suggested by Dimitrov et al. [25]. This model is also based on MD simulation. As detailed below, the kinetics of the fluid penetration through nanopores was assessed with the aid of the MD simulation code developed by Dimitrov et al. [25], and then the applicability of the hydrodynamic and MK models to derivation of the DCA was evaluated. In this investigation, we deal with the capillary imbibition of a polymer at a designed nanopore. In addition, an interesting result regarding the role of the wall–polymer interaction in the capillary imbibition process will be presented.

Model and MD simulation description

The model employed in this study is comprised of a cylindrical nanotube with the radius R=10. The capillary wall is presented by the atoms of a triangular lattice, which has a lattice constant 1.0 in units of the fluid atom diameter σ. The atoms of the capillary wall can fluctuate around their equilibrium positions at $R+\sigma$, corresponding to a finitely extensible nonlinear elastic potential (i.e., U_{FENE}) as follows:

$$U_{\mathrm{FENE}} = -15\varepsilon_{\mathrm{w}}R_0^2 \ln\left(1 - \frac{r^2}{R_0^2}\right) \tag{8}$$

where ε_{w} is the depth of the potential well, R_0 is a constant (R_0=1.5), and r is the distance between any pair of wall atoms. In the above equation, ε_{w} is defined as follows:

$$\varepsilon_{\mathrm{w}} = 1.0k_{\mathrm{B}}T \tag{9}$$

where k_{B} stands for the Boltzmann constant and T is the temperature of the system. In addition, it is assumed that the wall atoms interact by a Lennard–Jones (LJ) potential as follows:

$$U_{\mathrm{LJ}}(r) = 4\varepsilon_{\mathrm{ww}}\left[\left(\frac{\sigma_{\mathrm{ww}}}{r}\right)^{12} - \left(\frac{\sigma_{\mathrm{ww}}}{r}\right)^{6}\right] \tag{10}$$

where $\varepsilon_{\mathrm{ww}}$ and σ_{ww} are the depth of the potential well and the effective molecular diameter, respectively, which are determined to be $\varepsilon_{\mathrm{ww}}$=1.0 and σ_{ww}=0.8. Therefore, it is ensured that no penetration of fluid particles through the wall occurs. The right side of the capillary tube is closed by a hypothetically impenetrable wall, which holds the fluid particles inside the tube. The left side of the capillary tube is attached to a rectangular reservoir 40×40 involving fluid particles with periodic boundaries perpendicular to the tube axis. To avoid entry of the fluid particles into the tube before commencement of the MD simulation runs, the capillary wall is assumed to be completely hydrophobic. Therefore, the fluid particles remain in the reservoir as a stable fluid film. At time t=0, set to be the onset of capillary filling, the hydrophobic wall–polymer interactions are changed to hydrophilic ones and then the fluid enters the tube. At the same time, the structural and kinetic properties of the imbibition process are measured at equal intervals of time. In all simulation runs, a maximum capillary length of H_{max}= 55 is used. In order to integrate the equations of motion, the Verlet algorithm [26] is employed, and the temperature is kept constant using a DPD thermostat [27] with a friction parameter of ξ=0.5, Heaviside-type weight functions, and a thermostat cutoff of r_{c}=2.5σ. The integration time step δt is obtained by the following expression:

$$\delta t = 0.01t_0 \tag{11}$$

where t_0 is the basic time unit, which is obtained by the following equation:

$$t_0 = \sqrt{\frac{m\sigma^2}{48k_{\mathrm{B}}T}} \tag{12}$$

where m and $k_{\mathrm{B}}T$ are chosen to be 1.

Here, our simulation is restricted to a polymer consisting of short chains of length N=10. The bonded forces between the chain monomers result from a combination of the aforementioned FENE and LJ potentials with ε=1.0 [28]. However, the wall–polymer interaction is regarded as a variable parameter, which is given by an LJ potential with strength $\varepsilon_{\mathrm{WL}}$. To reduce the computation time, all interactions are cut off at r_{c}=2.5σ. The total number of fluid particles is 25,000, while those forming the tube are 3,243.

To determine the surface tension and viscosity of the polymer, following Ref. [29] for the polymer (at density ρ_{l}=1.043), it is found that η≈205±25. A compatible value for the viscosity is derived by applying an equilibrium MD simulation and then using the correlation function of the diagonal pressure tensor components and the standard Kubo relationship [26]. From the flat gas–fluid interface observed in the left side of our model, it is feasible to estimate the surface tension γ_{lv} from the anisotropy of the pressure tensor components [30] as follows:

$$\gamma_{\mathrm{lv}} = \int \left[p_{zz}(z) - \frac{p_{xx}(z) + p_{yy}(z)}{2}\right] \mathrm{d}z \tag{13}$$

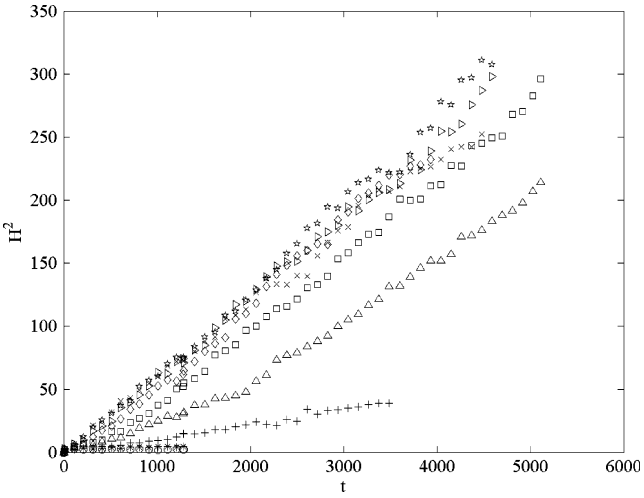

Fig. 2 Plot of the squared height of wetting as a function of the time in the case of imbibition of a designed nanopore by a polymer for the wall–polymer interactions 0.8 (○), 1.0 (*), 1.2 (+), 1.4 (Δ), 1.6 (□), 1.8 (◇), 2.0 (▷), 2.2 (☆), and 2.4 (×)

The above equation yields $\gamma_{lv}=1.715\pm0.025$ for the polymer.

As mentioned previously, the interaction strength between the polymer and the wall is considered as a variable in our MD simulations since it has been proved that this parameter has a crucial influence on the imbibition process at nanoscale. By varying this interaction strength, the wetting behavior of the test fluid can be achieved in a wide range.

Note that the MD simulation described above does use the dimensionless or reduced MD units to define all physical quantities, including the nanoscale dimensions. There are several reasons for doing this. One can refer to Ref. [31] to know more detail. One reason for using such units is related to the general notion of scaling, namely, that a single model can describe a whole class of problems. In the other words, when the properties of a given system have been measured in dimensionless units, they can readily be scaled to the meaningful physical units for each problem of interest.

Results and discussion

Figure 2 shows the time evolution of the squared height of wetting. It implies that the length of imbibition depends very sensitively on the strength of the wall–polymer interaction. The simulation results are also summarized in Table 1. This table indicates the correlation of the squared length of imbibition as a function of time for different ε_{WL} values in terms of a statistical parameter, namely, the squared correlation coefficient (R^2). The R^2 statistic is used almost universally in judging regression equations [32]. This statistic measures the correlation between the target values and those predicted by a given model. The square of correlation coefficient can take on any value between 0 and 1, with a value closer to 1 indicating that the model yields a greater fitness. As can be seen from this table, for $\varepsilon_{WL}=0.8$ and 1.0, a good correlation is not achieved. These cases yield $R^2=0.0471$ and 0.0874, respectively. However, for all other values of ε_{WL}, a very good relationship between the squared length of imbibition and the time, ranging from $R^2=0.9595$ to 0.9961, is obtained. Incidentally, in the latter ε_{WL} values (i.e., $\varepsilon_{WL}=1.2$ to 2.4), the accuracy of the LW equation is confirmed, whereas in the former choices of ε_{WL} (i.e., $\varepsilon_{WL}=0.8$ and 1.0), the simulation results do not obey the simple LW equation, and a modification of this equation is needed. Notice that only the contact angle (static or dynamic) varies in the LW equation. From Fig. 2, it is evident that there is an inverse relationship between the wall–polymer interaction and the contact angle since for the cases $\varepsilon_{WL}\geq1.6$, all simulation data, with a good approximation, fall in the same region. This implies that complete wetting (i.e., $\cos\theta=1$) occurs for those cases. As a result, a partial wetting of the nanopore for $\varepsilon_{WL}\leq1.4$ can be anticipated.

In what follows, the reason for this observed discrepancy between the results of MD simulation and the LW equation is examined. First, the inertia effect in our simulations is assumed to be small since the effect of inertia, which was initially proposed by Rideal [33] and Bosanquet [34], is only significant in the early stages of penetration or when the capillary radius is large and/or the viscosity of liquid is small. Therefore, this effect is ignored in the analysis of the simulation results. In addition, the influence of gravity is also negligible since the length of the nanotube is sufficiently short to take this parameter into consideration. As mentioned previously, this observed deviation from the LW equation is a result of neglecting the DCA. In order to demonstrate this fact, we should verify that the MD simulation results are in good agreement with the LW equation considering the DCA where the simple LW equation is not valid (i.e., $\varepsilon_{WL}=0.8$ and 1.0). To this end, we employed both hydrodynamic (i.e., Eq. 3 along with the

Table 1 Correlation of the squared wetting length as a function of time in the case of imbibition of a polymer into a designed nanopore for various wall–polymer interactions (ε_{WL}) in terms of the squared correlation coefficient (R^2)

ε_{WL}	0.8	1.0	1.2	1.4	1.6	1.8	2.0	2.2	2.4
R^2	0.0471	0.0874	0.9820	0.9595	0.9860	0.9879	0.9938	0.9961	0.9948

Cox equation) and MK (i.e., Eq. 7) models to obtain the DCA and to correlate the DCA as a function of the imbibition rate using the MD simulation data. The results of this investigation are summarized in Table 2, where it can be seen that for ε_{WL}=0.8 and 1.0, R^2=0.0230 to 0.1544 can be achieved. This result justifies that both hydrodynamic and MK models are not able to describe the kinetics of polymer penetration at nanopores where the simple LW equation tends to break down. Hence, a new model to tackle this problem is needed.

To explain why this nonconformity occurs, the theoretical background of these models is reexamined. Since the MK model does not include the viscous dissipation, it is not surprising that the model does not fit well with the computationally achieved data set of the capillary imbibition of the polymer having a high viscosity. On the other hand, the hydrodynamic model yields the better conclusions (i.e., R^2=0.1358 and 0.1544) compared with those calculated by the MK model (i.e., R^2=0.0273 and 0.0230). However, these values are not still acceptable since the Cox equation was developed to deal only with low capillary numbers where the hydrodynamic model gives reasonable slip length values. Capillary number Ca is given by Ca=$\eta v/\gamma_{lv}$, where v is the velocity of imbibition. The slip length is in the order of molecular dimensions only for a small range of capillary numbers (i.e., Ca=0.005–0.1) [35]. This limit, however, is not universal. For instance, Petrov et al. [36] reported a Ca=0.002 in which the hydrodynamic model is valid but they did not observe an upper limit for capillary numbers to apply to the hydrodynamic model. Therefore, further investigations are needed to confirm this limit. In the present case, for ε_{WL}=0.8 and 1.0, Ca=0.1391 and 0.1935, respectively, can be calculated, which are not in the range of the acceptable Ca for the hydrodynamic model. Intriguingly, a recent experimental study pertaining to the contact angle dynamics of the water droplets on surfaces with various wetting properties showed that even for a single liquid there is no universal expression to relate the contact angle with the contact-line speed [37].

Table 2 Correlation of the dynamic contact angle as a function of the wetting rate taken from the hydrodynamic and molecular–kinetic models in the case of imbibition of a polymer into a designed nanopore for various wall–polymer interactions (ε_{WL}) in terms of the squared correlation coefficient (R^2)

Model type	ε_{WL}	R^2
Hydrodynamic	0.8	0.1358
Hydrodynamic	1.0	0.1544
Molecular–kinetic	0.8	0.0273
Molecular–kinetic	1.0	0.0230

It is interesting to say that recently we performed the same simulation procedure in the case of a simple fluid (i.e., an LJ fluid) [38]. For this fluid, it was shown that generally the simple LW equation is a reliable model to explain the kinetics of the capillary wetting phenomenon. However, nonconformity to this equation was observed in some cases (i.e., small wall–fluid interactions) since the simple LW equation overlooks the significant effect of the DCA on this phenomenon. In addition, it was demonstrated that the LW equation together with a hydrodynamic model (i.e., the Cox equation) are able to justify the simulation results for those cases, which are not in good agreement with the simple LW equation. Note that these equations (i.e., the simple LW equation in association with the Cox equation) are not able to fit the simulation results in the case of polymer penetration inside the nanochannel. In order to explain this observed difference between a simple fluid and a polymer, let us compare the characteristics of both fluids. Intriguingly, it is found that the polymer has a higher viscosity (i.e., $\eta\approx205\pm25$) than that of the LJ fluid (i.e., $\eta\approx6.34\pm0.15$). Knowing that the viscosity of fluid is a measure of interaction between fluid particles [39], it can be concluded that the fluid–fluid interactions affect the imbibition of nanochannels much more than do the wall–fluid interactions where the interaction between wall and fluid is weak. Moreover, generally, it was found that higher viscosity of a fluid (i.e., higher fluid–fluid interaction) leads to slower wetting rate of nanochannels.

In what follows, we would like to demonstrate an interesting fact taken from our MD simulation results. As can be seen from Fig. 2, there is a direct relationship between the wall–polymer interaction and the speed of the capillary imbibition. This corollary is in contrast with this idea that the rate of the capillary imbibition is a non-monotonic function of the solid–liquid interaction [21, 24, 40]. The latter idea, which is based on the MK model, says that the strong solid–liquid interaction will have two opposing effects: increasing the driving force for the wetting (i.e., the out-of-balance surface tension force $\gamma_{lv}(\cos\theta_e-\cos\theta_d)$), but also increasing the resistance to the wetting due to reducing the general mobility of molecules within the three-phase zone. The mathematical proof of this issue and related supporting evidence can be found in the literature [21]. As a result, the maximum velocity at which a liquid can wet a solid depends in a non-monotonous way on substrate wettability [40]. The verification of this idea has been presented in the case of the imbibition at nanopores using MD simulation approach. We claim that this conclusion is not correct in general. It is true as long as the LW equation associated with the MK model is able to describe the kinetics of the imbibition. As verified previously, it happens when we confront the partial wetting of a given system. In all other cases, the LW equation is sufficiently enough to explain the kinetics of the imbibition.

Now, let us briefly review the latter case (i.e., Ref. [24]). They performed the large-scale molecular dynamics simulations to study the details of liquid imbibition into a cylindrical pore. The intramolecular interactions were considered to be the LJ type. By changing the strength of the wall–fluid interactions, they were able to vary the wettability of the nanopore. The dynamics of liquid imbibition were followed for two pores of different radii: 50 and 70 Å. During imbibition, the distance of meniscus penetration and the relaxation of the dynamic contact angle toward equilibrium as a function of time were measured. For both cases (i.e., the pore radii 50 and 70 Å), they found the imbibition speed of the nanopore is a nonlinear function of the fluid–solid interaction. The values of the wall–fluid interaction were determined to be ε_{WL}=0.8, 1.0, and 1.5, and it was claimed that the case ε_{WL}=1.0 corresponds to the maximum speed of the wetting. The main flaw of this work is that the consistency of the simple LW equation has not checked. More precise assessment of the MD simulation data in this work shows that for both cases ε_{WL}=1.0, and 1.5 complete wetting occurs since simulation data, with a good approximation, fall in the same region (see Figs. 5 and 6 in Ref. [24]). In addition, authors reported an equilibrium contact angle 0 for both cases (see Table 2 in Ref. [24]). Consequently, this result that there is an optimum liquid to achieve the most rapid imbibition is questionable. Now, let us present more evidence to support this claim that there is a direct relationship between the wall–polymer interaction and the speed of the capillary imbibition. First, it is interesting to say that this conclusion is in consonance with the recent work of Caupin et al. [41]. They tried to find an answer for this question that, what is the maximum possible capillary rise for a specific fluid? They considered the imbibition of various fluids at two different geometries, a slit pore, and a cylindrical pore and performed explicit calculations for the graphite and MgO substrates. It was found that there is a direct relationship between the maximum height of capillary rise and the fluid–surface interactions. Second, a recent experimental study of the penetration of polymer melts inside nanochannels showed that higher solid–liquid interaction between the melts and the surface leads to more noticeable flow of the polymer melts in the nanochannels [42].

Conclusions

MD simulation of imbibition of a polymer through a designed nanopore was carried out, and the following conclusions were obtained:

1. Generally, the simple LW equation is a reliable model to explain the kinetics of this phenomenon. However, nonconformity to this equation is observed in some cases since the simple LW equation overlooks the significant effect of the DCA on this phenomenon.
2. Two commonly used models to derive the DCA, namely, the hydrodynamic and MK models, were proposed. However, the results showed that none of the evaluated models is able to justify the simulation results in which are not in good agreement with the simple LW equation.
3. Further investigation of the MD simulation data revealed an interesting fact that there is a direct relationship between the wall–polymer interaction and the speed of the capillary imbibition.

Acknowledgments S. Ahadian greatly appreciates Dr. Dimitrov, Professor Milchev, and Professor Binder. The authors sincerely appreciate the staff of the Center for Computational Materials Science of the Institute for Materials Research (IMR), Tohoku University, for its continuous support of the supercomputing facilities. This work was supported (in part) by the Japan Society for the Promotion of Science (JSPS).

References

1. Shin K, Obukhov S, Chen JT, Huh J, Hwang Y, Mok S, Dobriyal P, Thiyagarajan P, Russel TP (2007) Nat Mater 6:961–965
2. Li H, Ke Y, Hu Y (2006) J Appl Polym Sci 99:1018–1023
3. Suh KY, Kim YS, Lee HH (2001) Adv Mater 13:1386–1389
4. Stafford CM, Harrison C, Beers KL, Karim A, Amis AJ, VanLandingham MR, Kim HC, Volksen W, Miller RD, Simonyi EE (2004) Nat Mater 3:545–550
5. Lucas R (1918) Kolloid-Z 23:15–22
6. Washburn EW (1921) Phys Rev 17:273–283
7. Supple S, Quirke N (2003) Phys Rev Lett 90:214501
8. Supple S, Quirke N (2005) J Chem Phys 122:104706
9. de Gennes PG (1985) Rev Mod Phys 57:827–863
10. Cox RG (1986) J Fluid Mech 168:169–194
11. Shikhmurzaev YD (1997) J Fluid Mech 334:211–249
12. Blake TD, Haynes JM (1969) J Colloid Interface Sci 30:421–423
13. Martic G, Blake TD, De Coninck J (2005) Langmuir 21:11201–11207
14. Bracke M, De Voeght F, Joos P (1989) Prog Colloid Polym Sci 79:142–149
15. Voinov OV (1976) Fluid Dynamics 11:714–721
16. de Gennes PG, Hua X, Levinson P (1990) J Fluid Mech 212:55–63
17. Thompson PA, Robbins MO (1989) Phys Rev Lett 63:766–769
18. Cazabat AM, Gerdes S, Valignat MP, Villette S (1997) Interface Sci 5:129–139
19. Cherry BW, Holmes CM (1969) J Colloid Interface Sci 29:174–176
20. Ruckenstein E, Dunn CS (1977) J Colloid Interface Sci 59:135–138
21. Blake TD, De Coninck J (2002) Adv Colloid Interface Sci 96:21–36
22. Blake TD (2006) J Colloid Interface Sci 299:1–13
23. Martic G, Gentner F, Seveno D, Coulon D, De Coninck J, Blake TD (2002) Langmuir 18:7971–7976
24. Martic G, Gentner F, Seveno D, De Coninck J, Blake TD (2004) J Colloid Interface Sci 270:171–179
25. Dimitrov DI, Milchev A, Binder K (2007) Phys Rev Lett 99:054501
26. Allen MP, Tildesley DJ (1987) Computer simulation of liquids. Clarendon, Oxford
27. Soddemann T, Dünweg B, Kremer K (2003) Phys Rev E 68:046702
28. Grest GS, Kremer K (1986) Phys Rev A 33:3628–3631

29. Backer JA, Lowe CP, Hoefsloot HCJ, Iedema PD (2005) J Chem Phys 122:154503
30. Rowlinson JS, Widom B (1982) Molecular theory of capillarity. Clarendon, Oxford
31. Rapaport DC (2004) The art of molecular dynamics simulation (chapter 2), 2nd edn. Cambridge University Press, Cambridge
32. Draper NR, Smith H (1998) Applied regression analysis, 3rd edn. Wiley, New York
33. Rideal EK (1922) Phil Mag 44:1152–1159
34. Bosanquet CH (1923) Phil Mag 45:525–531
35. Ranabothu SR, Karnezis C, Dai LL (2005) J Colloid Interface Sci 288:213–221
36. Petrov JG, Ralston J, Schneemilch M, Hayes RA (2003) Langmuir 19:2795–2801
37. Bayer IS, Megaridis CM (2006) J Fluid Mech 558:415–449
38. Ahadian S, Kawazoe Y (2009) Mater Trans 50:1157–1160
39. Karniadakis G, Beskok A, Aluru NR (2005) Microflows and nanoflows: fundamentals and simulation, 2nd edn. Springer, New York
40. Blake TD, De Coninck J (2004) Colloids Surf A: Physicochem Eng Asp 250:395–402
41. Caupin F, Cole MW, Balibar S, Treiner J (2008) Eur Phys Lett 82:56004
42. Yung KL, Kong J, Xu Y (2007) Polymer 48:7645–7652